The Anti-Diabetic Effect of Nano-Encapsulated Propolis from *Apis mellifera* on Type 2 Diabetes

Sarah S. Hegazy[1]*, Hanan Helmy[2], Mohamad S. Salama[1], Nadia M. Lotfy[1] and Dalia M. Mahmoud[1]

[1]Entomology Department, Faculty of Science, Ain Shams University, Cairo, Egypt
[2]Research and Training Center on Vectors of Disease, Ain Shams University, Cairo, Egypt

Received: 28 March 2020, Revised: 22 July 2020, Accepted: 10 August 2020

Abstract

Diabetes mellitus is viewed as a major disease and is among the most prevalent health problems globally. The goal of the present research was to evaluate the therapeutic efficiency of an ethanolic extract of Egyptian propolis (EEP) conjugated with chitosan polyacrylic (CS-PAA) nanoparticles against type 2 diabetes mellitus. Thirty Wistar rats were randomly categorized into 6 groups (5 animals/ group). Group I consisted of normal rats as a normal control. The remaining five groups were injected with streptozotocin (STZ), a diabetogenic agent, in order to induce diabetes. The experimental groups were treated for 4 consecutive weeks as follows: Group II included untreated diabetic rats, serving as a negative control. Group III consisted of diabetic rats treated with EEP. Group VI consisted of diabetic rats treated with Metformin. The findings of this work illustrated that no significant differences were noticed concerning the body weight of the treated groups compared to that of the normal control group. Blood glucose levels were significantly decreased in the diabetic rats treated with EEP and EEP encapsulated CS-PAA nanoparticles compared to the untreated diabetic rats. The results indicated that EEP encapsulated CS-PAA nanoparticles displayed a potential therapeutic effect against type 2 diabetes mellitus.

Keywords: diabetes mellitus; chitosan, polyacrylic acid; propolis; body weight
DOI 10.14456/cast.2021.11

1. Introduction

Diabetes is viewed as a chronic metabolic disease marked by high blood sugar (hyperglycemia) and is a leading global health problem. In addition, it is one of the most distressing medical problems of the century. Per the data described by the World Health Organization **(**WHO**)**, the global incidence rates of diabetes mellitus were 171,000,000, and this number is predicted to escalate up to 439,000,000 by 2030. Diabetes mellitus is distinguished by a deficiency regarding insulin secretion and/or action, associated with chronic hyperglycemia and disorders of carbohydrate, protein, and lipid metabolism [1].

Propolis is defined as a resinous substance gathered and produced by honeybee workers from various floral substances along with bees wax and salivary secretions. One of the unique

*Corresponding author: Tel.: (+20) 100 494 2997
E-mail: sarah.hegazy@sci.asu.edu.eg

characteristics of propolis is its high resin content (approx. 50%), in addition to wax (30%), essential oils, pollens, along with other organic components [2]. Noticeably, propolis composition differs according to its geographical area of origin, in addition to the type of flora in that region. Propolis, in particular, possesses an extensive variety of biological activities, including antioxidant, antiviral, anti-inflammatory, cytotoxic, antimicrobial, and immune-modulatory properties. In addition, some recent studies have revealed that propolis has hypoglycemic properties in addition to antioxidant capacity [3]. Preceding studies revealed that ethanol and water extracts of propolis exhibited positive effects in diabetic animals [4].

Nanoparticles have been used since the early 1990s. They have been used as drug delivery vehicles either by encapsulating the drugs or by the deposition of the drugs on the surface of the nanocarrier molecules [5]. Nonetheless, polymeric nanoparticles and liposomes are among the most recognized delivery vehicles of drugs with medical applications in the pharmaceutical area. Polymeric nanoparticles have achieved this standing due to their biocompatibility, non-toxicity to biological systems, biodegradability, long shelf life, controlled release, targeted delivery and therapeutic efficiency [6].

There has been a disastrous rise in diabetes across the world, paralleling the prevalence of obesity. More than 95 percent of obese/overweight people would develop type-2 diabetes (T2D) during their lifetime [7]. Moreover, the type-2-diabetic drug, metformin is being investigated for traces of a probable carcinogen in addition to other side effects hampering its therapeutic efficiency [8]. Consequently, it is an excessive insistence to find alternative treatments and innovative inhibition tactics for T2D. The present study investigated the effect of encapsulated propolis on the body weight and blood glucose level of type 2 diabetic rats.

2. Materials and Methods

2.1 Preparation of propolis samples

Egyptian propolis samples were harvested from local western honey bee workers (*Apis mellifera* Linnaeus) from Egyptian bee colonies located at the Agriculture Research Centre at Dokki, Giza Governorate, Egypt, according to the method of Souza *et al*. [9], using glass slides close to the internal and lateral walls of the rearing boxes.

The collection process involved using white glass slides (48 cm length, 5 cm width and 5 mm thickness), arranged contiguously to each other and put onto the top bar of the rearing combs, with an elevation at approximately 3 mm in between.

2.1.1 Preparation of ethanolic extract of propolis

The ethanolic extract of propolis (EEP) was formulated by the maceration of raw propolis at room temperature, usually accompanied by shaking, in the proportion of 10 g raw propolis to 100 ml of ethanol 80% (solvent). The propolis extracts were collected after 7 days of maceration and filtration by Whatman No. 1 filter paper per the procedure reported by Cunha *et al.* [10].

2.1.2 Characterization of propolis extract by Gas Chromatography-Mass Spectrometry (GC-MS)

The component detection was achieved using the database and software of the National Institute Standard and Technology (NIST) and Wiley Registry of Mass Spectral data's, New York (WILEY). The characterization data, including retention time and peak area percentages, were acquired using

th GC-MS chemical analysis to identify the major components present in the propolis sample. The components with percentage peak area greater than 0.07% were considered to be significant elements and were documented according to Usman *et al*. [11].

2.2 Preparation of nanoparticles

The chitosan**-**poly acrylic acid (CS-PAA) polymer was conjugated with the EEP according to the method of Braun *et al*. [12]. The CS-PAA nano-spheres were synthesized by polymerization. An amount of 100 g of chitin (Sigma Aldrich, USA) was converted to chitosan through a deacetylation process using 500 ml of saturated NaOH and glycerin bath at 160ºC-170ºC for 3 h [13]. Later the chitosan solution obtained was mixed with polyacrylic acid solution with stirring overnight.

The polymerization was accomplished by preheating 22 ml of distilled water to 70°C, with an inlet for nitrogen flow, and another one for a thermometer. At this temperature, a solution of potassium persulphate (KPS) (0.32 g/8 ml distilled water to produce 0.66 mM solution) was slowly introduced dropwise into the flask over a period of 5-10 min, while stirring at 300 rpm. The saturated solution of the EEP was introduced into the acrylic acid (AA) and the cross-linking agent KPS to produce EEP conjugated with CS-PAA polymer. After complete polymerization was reached, the temperature was kept at 80°C for another 30 min. Afterwards, the viscous polymer solution was added dropwise to 0.1 N hydrochloric acid (HCl), whereupon the polymer precipitated. The polymer was then incubated for 48 h at 60ºC. The resulting polymer was dried to constant weight at 50°C. After the drying process, each of the resulting polymer formulations (blank and EEP-conjugated CS-PAA) was rod-milled thoroughly for 1 h using a home-made rod mill (100 rpm), then sonicated (42 KHz, 15 min, CE-7200A, China) and finally centrifuged (12,000 ×*g*, 30 min) to remove insoluble materials. The nano-spheres were powdered by freeze-drying at -44ºC (LGJ-18C, China).

2.3 Characterization of the propolis conjugated with nanoparticles

2.3.1 Physicochemical characterization of the CS-PAA nanoparticles

Examination of propolis conjugated with nanoparticles by Transmission Electron Microscopy (TEM) was done according to Ray *et al*. [14] and Wang *et al*. [15]. Samples were sonicated for 30 min (42 KHz, CE-7200A, China) prior to being loaded on a TEM sample grid (silicon oxide supported by copper mesh) via standard fine tweezers. Afterward, the loaded TEM grids were left to dry in air.

The size distribution and mean diameter of the CS-PAA nanoparticles (hollow and EEP-loaded) were measured by dynamic light scattering (DLS) (Zetasizer 3000 HS, Malvern, UK) in pH 4 buffer solution according to the method described by Kao *et al*. [16]. The nanoparticles' samples were diluted, and then the DLS measurements were done with a wavelength of 633 nm at 25ºC with an angle detection of 90º**.** The measurements were done in triplicates and the mean diameter ± SD was calculated**.**

2.3.2 Determination of the EEP encapsulation efficiency of the CS-PAA nanoparticles

The amount of EEP encapsulated into the CS-PAA nanoparticles was calculated by determining the difference between the total EEP amount used to prepare the nanoparticles and the amount of EEP present in the aqueous phase, according to the method described by Andrade *et al*. [17].

After the preparation, the EEP-loaded nanoparticles were separated from the aqueous suspension medium by centrifugation at 50,000 ×*g* for 2 h. After centrifugation, the amount of free propolis in the clear supernatant was measured using a UV spectrophotometer (LS-50B, Perkin

Elmer) at the wavelength of 425 nm. All analyses were carried out in triplicates and blank nanoparticles were used as control. Encapsulation efficiency was calculated using equation (1).

$$\text{Encapsulation Efficiency} = \frac{\text{Total amount of propolis} - \text{Free amount of propolis}}{\text{Total amount of propolis}} \times 100 \quad (1)$$

2.3.3 *In vitro* release of propolis from the CS-PAA nanoparticles

The release of propolis from CS**-**PAA nanoparticles was carried out in an aqueous phosphate buffer solution at pH 4 (to simulate the gastric environment) and 37◦C, according to Zhu *et al*. [18]. The EEP**-**loaded nanoparticles were placed into 60 ml of aqueous buffer solution. Each 10 min, 3 ml samples of the aqueous buffer solutions were withdrawn and replenished by 3 ml fresh buffer solution to maintain a constant volume. The amount of the released propolis in the withdrawn buffer samples was determined by UV-vis absorbance at 425 nm. All EEP release data were performed in triplicate and averaged. The release percentage of the propolis was plotted against time in minutes.

2.3.4 Fourier transform infrared (FT-IR, Thermo Nicolet 6700, UK) spectroscopy

This technique was applied according to Ray *et al*. [14] and Wang *et al*. [15] to determine the chemical structure and functional groups of surface-modified nanoparticles revealing interactions at the nanoparticle surface.

The procedure involved taking FT-IR spectra of CS-PAA polymer and propolis conjugated with CS-PAA using the potassium bromide (KBr) pellet technique, which involved crushing the different samples in a mortar, then mixing each of the crushed materials with KBr (IR spectroscopy grade). Afterwards, the mixture was compressed to 12 mm diameter semi-transparent disk by applying a pressure of 65 kN (pressure gauge, Shimadzu, China) for two min. The FT-IR was verified in the range of 400-4000 cm^{-1} via FT-IR spectrophotometer. To know if there was any chemical interaction between propolis and polymer nanoparticles, IR spectra of the previously mentioned specimens were compared together.

2.4 The experimental induction of diabetes

The rats, serving as the experimental study samples, were procured from the lab animals house at the medical research center (MRC), Ain Shams University, and then were divided into two main groups, experimental or treatment and control. The induction of type-2 diabetes (T2D) in the studied rats was achieved by intoxicating their pancreatic β-cells using streptozotocin (STZ), a potent diabetogenic agent.

The rats (treatment and control) were allowed a standard formulated pellet diet and water access, *ad libitum*, during the duration of the experiment and were maintained at 24 ± 2◦C, 60-70% humidity, <50 dB noise level, and 12 h dark/12 h light cycles. All animal maintenance and experimentation procedures were done in accordance with the Ethical Principles of Animal Research adopted by the Faculty of Science, Ain Shams University.

In this study, a mixture of high fat diet (HFD) for 2 weeks and a single dose intraperitoneal injection (35 mg/ kg STZ) for 3 successive days were used to induce T2D in the rat models according to Vatandoust *et al*. [19]. The components of the HFD diet (as a percentage of total kcal) were 41% fat, 18% protein, and 41% carbohydrates. Rats were fed on their corresponding diets for 2 weeks before injection of STZ, according to Dranse *et al*. [20]. The STZ agent was dissolved in a sterile biological citrate buffer (0.05 M, pH 4.5). After 72 h, all rats were fasted for 16 h and their blood glucose levels were checked from the tail vein using a glucose analysis kit and an auto-analyzer (ACCU-CHEK Active, Roche diagnostics). After 1 week of the last STZ injection, the blood of the

studied groups was collected from the caudal vein (groups II-VI) in a fasting state. After plasma separation, an aliquot was taken for the measurement of insulin by ELISA test (Linco Research, Inc), to confirm the development of T2D (evident by insulin resistance) [21, 22]. The rats used in the experiments were regarded as diabetic when their fasting blood glucose (FBG) levels were more than 200 mg/dl [23]. The treatment was made available to the diabetic study sample through an oral gavage, on a daily basis for 30 days.

2.4.1 Experimental design

Male Wister albino (30) rats were used in this research and categorized into 6 groups (5 animals/ group), as follows:
Group I: Included non-diabetic rats that received only 0.9% NaCl saline solution as a normal control.
Group II: Included diabetic rats without treatment as a negative control.
Groups III: Included diabetic rats treated with EEP at dosage levels of 300 mg/kg.
Groups IV: Included diabetic rats treated with CS-PAA nanoparticles at dosage levels of 300 mg/kg.
Groups V: Included diabetic rats treated with EEP conjugated with CS-PAA nanoparticles at dosage levels of 300 mg/kg.
Groups VI: Included diabetic rats treated with Metformin (Met) at dosage levels of 100 mg/kg.

Bodyweight and blood glucose were recorded every week for diabetic- related measurements. The selected dose of propolis was according to the reported guidelines of Al-Hariri *et al*. [24] and Usman *et al*. [25].

2.4.2 Blood sampling and analysis

At the termination of the experiment, rats were fasted 14-16 h after their last meal, and then blood samples were harvested under diethyl-ether-induced anesthesia, from the heart of each rat. The blood samples were then centrifuged for 10 min at 2,000 ×*g* and 4°C, and afterwards, the serum was separated and stored at -80°C until further analysis.

2.5 Statistical analysis

Analysis of variance (ANOVA) and Tukey statistical tests were employed. Data were shown as means ± standard deviation ($P < 0.05$).

3. Results and Discussion

3.1 Gas chromatography-mass spectrometry (GC-MS)

The GC-MS spectrum of propolis extract confirmed the presence of a number of components, as illustrated in Figure 1. The peak numbers in Table 1 were designated according to the retention time of the major peaks, corresponding to the main 26 compounds identified and listed in Table 1. Flavonoids in propolis are classified into flavones, flavonols, flavanones, flavanonols, chalcones as 2'-Hydroxy-2,3,4',6'-tetramethoxychalcone, dihydrochalcones, according to their chemical structure, in addition to sugars (like fructose), mannitol, esters, and glycerol.

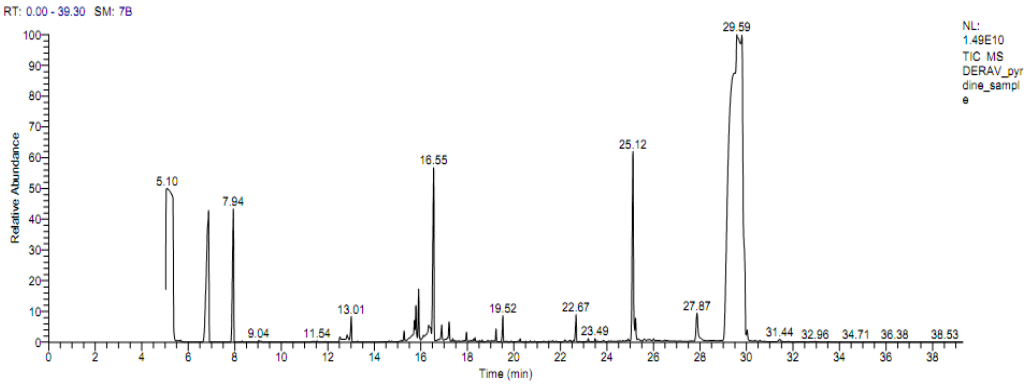

Figure 1. Gas chromatography-mass spectrometry (GC-MS) of ethanolic extract of propolis (EEP)

Table 1. Chemical composition of ethanol extracts of Egyptian propolis sample by GC-MS

Peak area (%)	Retention time (min.)	Compound name	Molecular formula	Molecular weight (u)
24.55	5.33	2-[3,4-(Methylenedioxy) Phenyl]-1-Cyclopentanone	$C_{12}H_{12}O_3$	204
		3(2h)-Pyridazinone, 4,5-Dihydro-4-(4-Methoxyphenyl)-	$C_{11}H_{12}N_2O_2$	204
		7-Methoxy-3,6-Dimethyl-2-Tetralone	$C_{13}H_{16}O_2$	204
		2'-Hydroxy-2,3,4',6'-Tetramethoxychalcone	$C_{19}H_{20}O_6$	344
8.95	6.87	4(Pentadeuterio)Phenylazulene	$C_{16}H_{12}$	204
		1[(Hexadeuterio)Phenyl]Naphthalene	$C_{13}H_{24}N_2$	208
		1h-Pyrrole, 2-(5-Chloro-2-Methoxyphenyl)-	$C_{16}H_6D_6$	210
5.47	7.93	Glycerol, Tris (Trimethylsilyl) Ether4	$C_{12}H_{32}O_3Si_3$	308
0.81	13.01	Sulfamic Acid, 3TMS Derivative Tris(Trimethylsilyl)Sulfamate	$C_9H_{27}NO_3SSi_3$	313
0.26	15.28	Levoglucosan, 3TMS Derivative Levoglucosan, Tris(Trimethylsilyl)-1H-INDOLE	$C_{15}H_{34}O_5Si_3$	378
1.26	15.91	D-Psicofuranose, Pentakis(Trimethylsilyl) Ether (Isomer 2)	$C_{21}H_{52}O_6Si_5$	540
0.43	16.34	Quinic Acid-Pentatms	$C_{22}H_{52}O_6Si_5$	552
		Chlorogenic Acid (6TMS)	$C_{34}H_{66}O_9Si_6$	786
6.85	16.55	9,9'(10h,10'h)-Spirobiacridine	$C_{25}H_{18}N_2$	346

Table 1. (cont.)

Peak area (%)	Retention time (min.)	Compound name	Molecular formula	Molecular weight (u)
0.67	17.21	3,6-Heptanooxepin-4,5-Dicar Bonsaure-Dimethylester	$C_{17}H_{22}O_5$	306
0.29	17.96	D-Glucopyranose, 5TMS Derivative	$C_{21}H_{52}O_6Si_5$	540
		Glucopyranose, 1,2,3,4,6-Pentakis-O-(Trimethylsilyl)-,		
0.31	19.23	Myo-Inositol, 6TMS Derivative	$C_{24}H_{60}O_6Si_6$	612
		Myo-Inositol, 1,2,3,4,5,6-Hexakis-O-(Trimethylsilyl)		
0.75	19.52	Caffeic Acid, 3TMS Derivative	$C_{18}H_{32}O_4Si_3$	396
		Trimethylsilyl3,4-Bis(Trimethylsiloxy)Cinnamate		
0.86	22.67	5á-Androstan-7á,17à-Dimethyl-3à,17á-Diol, Di-Trimethylsilyl	$C_{27}H_{52}O_2Si_2$	464
		Pregnan-11-One, 3,17,20-Tris[(Trimethylsilyl)Oxy]-, (3à,5á,20s)-	$C_{30}H_{58}O_4Si_3$	566
		Sucrose, 8TMS Derivative	$C_{36}H_{86}O_{11}Si_8$	918
0.61	25.23	Maltitol, Nonakis(Trimethylsilyl) Ether	$C_{39}H_{96}O_{11}Si_9$	992
		Cis-5-O-Feruloylquinic Acid, 5TMS	$C_{32}H_{60}O_9Si_5$	728
		17-Phenyl Trinor Prostaglandin E2	$C_{23}H_{30}O_5$	386
0.80	29.93	3-O-Coumaroyl-D-Quinic Acid, 5TMS	$C_{31}H_{58}O_8Si_5$	698
0.21	30.03	1,3-Benzodioxole, 3a,6,7,7a-Tetrahydro-2,2,3a,7-Tetramethyl-5 (Phenylsulfonyl),[3AS(3Aà,7á,7Aà)]	$C_{17}H_{22}O_4S$	322

The GC-MS analytical data demonstrated the existence of 26 compounds in Egyptian EEP. This result is to some degree in contrast with analysis of Malaysian propolis, which described 36 compounds by GC-MS analysis when extracted with ethanol. This difference may have been due to the fact that the chemical make-up of propolis is affected by the geographical locale, botanical origin, and bee species, according to Usman *et al.* [11].

The Egyptian EEP was found to be rich in phenolic compounds including cinnamic acid, caffeic acid, coumaric acid, and their derivatives. This result was in agreement with the study of Huang *et al.* [26] and that of Huang *et al.* [27].

3.2 Characterization and propolis-polymer biocompatibility

3.2.1 Physicochemical characterization, size distribution and encapsulation efficiency of EEP-loaded CS-PAA nanoparticles

The TEM photomicrographs elaborated the morphology of CS-PAA polymer and propolis conjugated CS-PAA nanoparticles. In addition, the size distribution (in terms of diameter) of the resultant propolis conjugated CS-PAA nanoparticles along with their topography was also revealed.

The blank CS-PAA polymer nanoparticles were shown to be approximately 24-32 nm spheres as illustrated in Figure 2a and Table 2.

The propolis conjugated CS-PAA polymer nanoparticles ranged in size between 40 nm and they were in the form of encapsulated spheres according to the data revealed by Figure 2b and Table 2. The encapsulation efficiency assay showed that propolis was efficiently core-encapsulated within the CS-PAA nanoparticles, evidenced by a 90.2 ± 2.3% encapsulation efficiency.

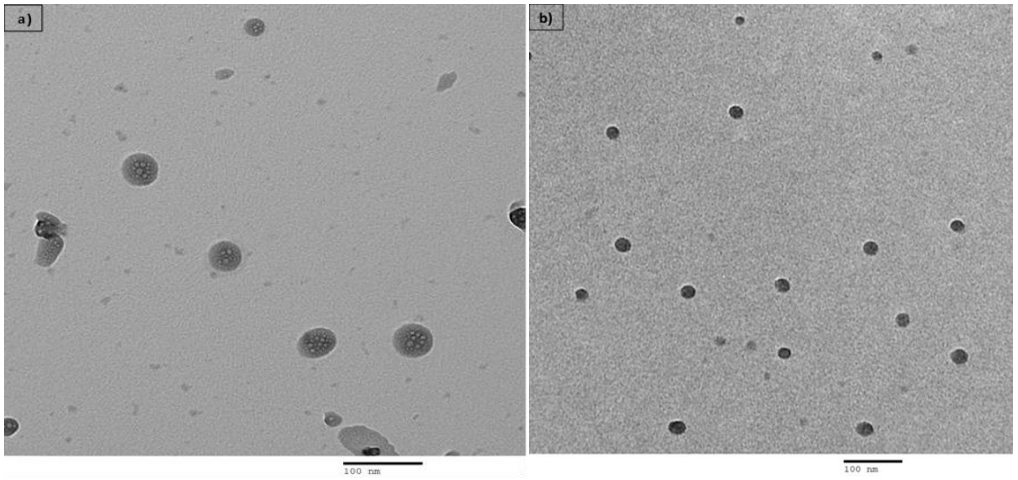

Figure 2. Transmission electron microscope micrograph showing a magnified view of the morphology and topography of: (a) the blank CS-PAA nanoparticles, size 24-32 nm; and (b) the EEP encapsulated in CS-PAA nanoparticles, size 40 nm

Table 2. Size distribution of the blank and EEP-loaded CS-PAA nanoparticles

	Hollow	**EEP-loaded**
Diameter of Nanoparticles (Mean ± SD)	29 ± 10	40 ± 12

The morphology and topography of the individual polymer and propolis conjugated nanoparticles was found to be regularly spherical with a diameter of 24-32 nm and around 40 nm, respectively. In addition, the propolis was observed to be encapsulated within the core of the CS-PAA nanoparticles at a level of 90.2 ± 2.3%. The encapsulated propolis was easily absorbed throughout the polymer matrix crystalline structures. These results are in agreement with Cevher *et al.* [28] and Seven *et al.* [29].

Additionally, this size range was in accordance with the study conducted by Omidirad *et al.* [30] on doxorubicin-loaded poly AA-coated magnetite nanoparticles, where the particles were 6-15 nm. On the other hand, this range was not in agreement with the study conducted by Guo *et al.* [31], in which the size range of the resulting EEP-loaded nanoparticles was between 1-100 nm. This discrepancy in the size range of the resulting particles may have been due to the variation in the synthesis process and type of the nanoparticles.

3.2.2 *In vitro* EEP release from CS-PAA nanoparticles

The *in vitro* release of EEP from the CS-PAA nanoparticles, as illustrated in Figure 3, showed that nearly 60% of the propolis payload was released within the first 800 min. The release profile involved a brief initial burst release in the first 40 min, followed by a slower release rate, and then another release burst was detected still within the first 200 min. Afterwards, the release occurred at a slow but constant rate. This observation could be due to a rapid degradation of the polymer outer shell in the first 40 min, followed by partial degradation of the initial CS layer beneath the PAA outer shell. These findings are in accordance with the study of Dounighi *et al.* [32].

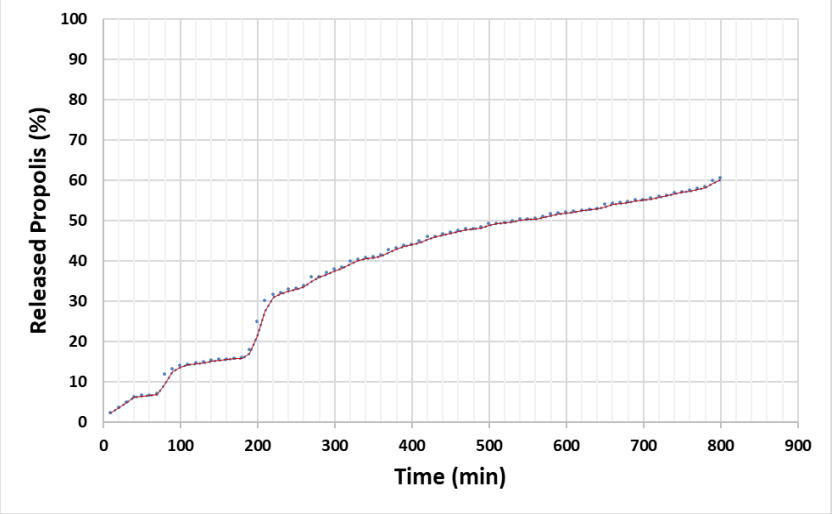

Figure 3. Propolis release profile from CS-PAA nanoparticles at pH 4

3.2.3 Fourier transform infrared (FT-IR)

Figure 4 showed the results obtained from the comparative FT-IR study between CS-PAA polymer, and propolis conjugated CS-PAA nanoparticles. The characteristic absorption bands of CS-PAA polymer displayed peaks in the 500, 1000, 1500, 2000, 2500, 3000 and 3500 cm^{-1} regions. The peaks shown by the propolis conjugated nanoparticles were found to be nearly identical to those produced by the blank CS-PAA polymer. The results showed a slight difference in the chemical group bands between CS-PAA polymer and EEP-conjugated CS-PAA nanoparticles.

The FT-IR data illustrated the appearance of spectroscopic peaks characteristic for the chosen parent polymer, CS-PAA, in the propolis conjugated CS-PAA samples without showing any traces for those characteristics for propolis (i.e. propolis was completely masked). This result strongly suggests the complete and successful physical encapsulation of propolis by CS-PAA without forming any chemical bonding. Otherwise, the chemical conformations of the polymer and the encapsulated propolis would have been altered and this would have accordingly resulted in the appearance of new FT-IR peaks, different from those of both the polymer and propolis.

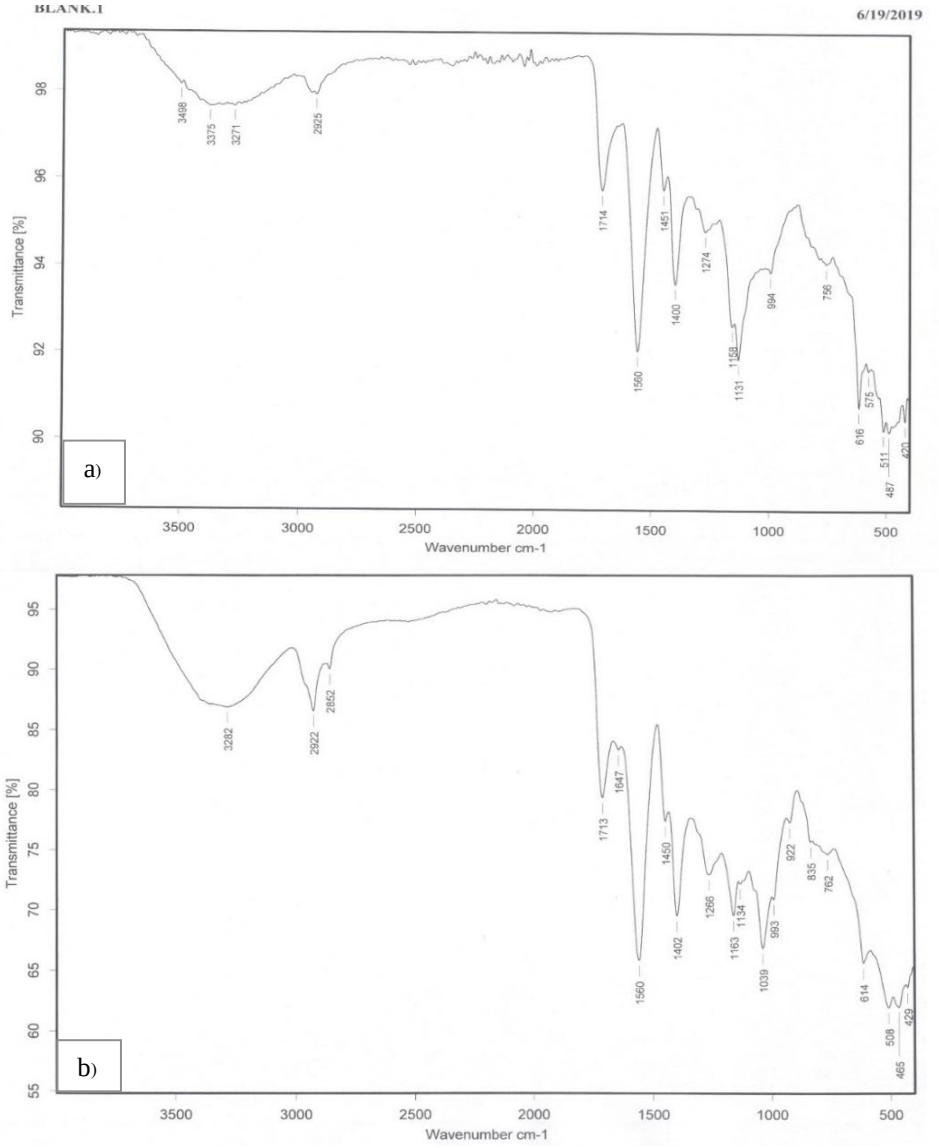

Figure 4. Fourier transforms infra-red spectrographs for (a) the CS-PAA polymer, and (b) the EEP-conjugated with CS-PAA polymer

For the pure propolis, the peaks produced were in the 400-4000 cm^{-1} regions according to Hussein *et al.* [33]. A comparison between the characteristic peaks was performed in the region of 2500-3500cm^{-1} to determine the efficiency of CS-PAA polymer nanoparticles encapsulation of propolis without any chemical interactions. Peres *et al.* [34] mentioned that the strong and broadband at 3445 cm^{-1} is associated with the −OH hydrogen bonds between the polyphenol rings.

3.3 Effect of EEP and EEP conjugated with CS-PAA nanoparticles on type 2 diabetes mellitus

3.3.1 The experimental induction of type-2 diabetes

The initiation of experimental T2D in the rats via diabetogenic chemicals is very convenient and simple to use, and a famous example of such chemicals is STZ. In the current work, induction of T2D via STZ at a dosage of 35mg/kg in rats was conducted according to El Rabey *et al.* [35], and the experimental animals showed a notable rise in the serum glucose levels in comparison to those in the normal control group. Moreover, the results of fasting serum insulin (FSI), evident in Table 3, illustrated that all the studied groups showed normal insulin range, with an emphasis that the groups II-VI showed lower values than the normal control (group I).

Table 3. Fasting serum insulin (FSI) for the studied rat groups

Weeks	Groups*					
	I	**II**	**III**	**IV**	**V**	**VI**
FSI (ng/ml) (Mean ± SD)	$1.12^{a} \pm 0.07$	$0.94^{a} \pm 0.04$	$1.01^{a} \pm 0.06$	$0.97^{a} \pm 0.03$	$0.88^{a} \pm 0.08$	$0.99^{a} \pm 0.06$

*Means that do not share a letter are significantly different.

3.3.2 Changes in body weight

Figure 5 shows the changes in bodyweight of the studied groups. The results did not show notable differences with respect to the body weight at the initiation of drug administration ($P>0.05$), however during the following 4 weeks of drug administration, the bodyweight of each studied group increased gradually. The bodyweight of all treated groups increased at an equal rate compared to the control groups.

Data revealed no marked differences with respect to the body weight of all the diabetes-afflicted groups compared to that of the normal control group. These findings came in agreement with those of Holmes *et al*. [36] and El Rabey *et al*. [35], who suggested that at the end of the study period, experimental rats weighed the same as the control rats.

3.3.3 Changes in blood glucose level

As shown in Figure 6, diabetic rats served as a negative control (group II) and showed increasing hyperglycemia from week 1 until week 4, whereas the groups of diabetic rats treated with EEP (group III) and EEP conjugated with CS-PAA (group IV) showed significantly reduced blood glucose levels from week 1 till the end of the treatment period. The group of diabetic rats treated with EEP conjugated with CS-PAA showed a three-fold significant decrease in blood glucose level compared to the diabetic positive control, EEP group and metformin group ($P < 0.05$). In the healthy rats, constant glucose levels were maintained below 200 mg/dl.

These results, combined with those of FSI values indicate that the type of diabetes developed in the diabetic rats (groups II-VI) is type 2, indicated by normal serum insulin accompanied with hyperglycemia, a strong indicator of insulin resistance [24].

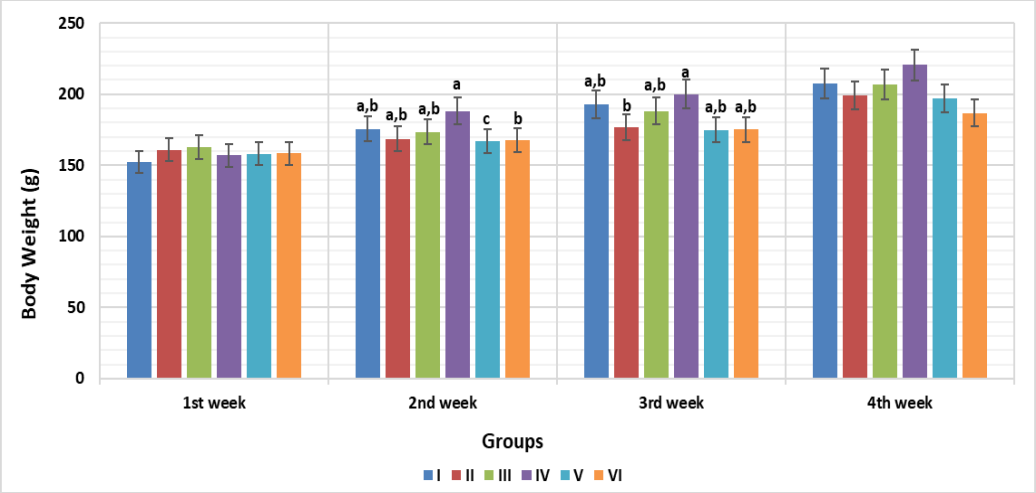

Figure 5. Changes in body weight (g) of rats with induced T2D and normal rats treated for 4 weeks after STZ administration where means that do not share a letter are significantly different. I: non-treated non-diabetic group (normal control), II: non-treated diabetic group (negative control), III: diabetic group treated with EEP, IV: diabetic group treated with CS-PAA nanoparticles, and V: diabetic group treated with (EEP) conjugated with (CS-PAA) nanoparticles, VI: diabetic group treated with metformin

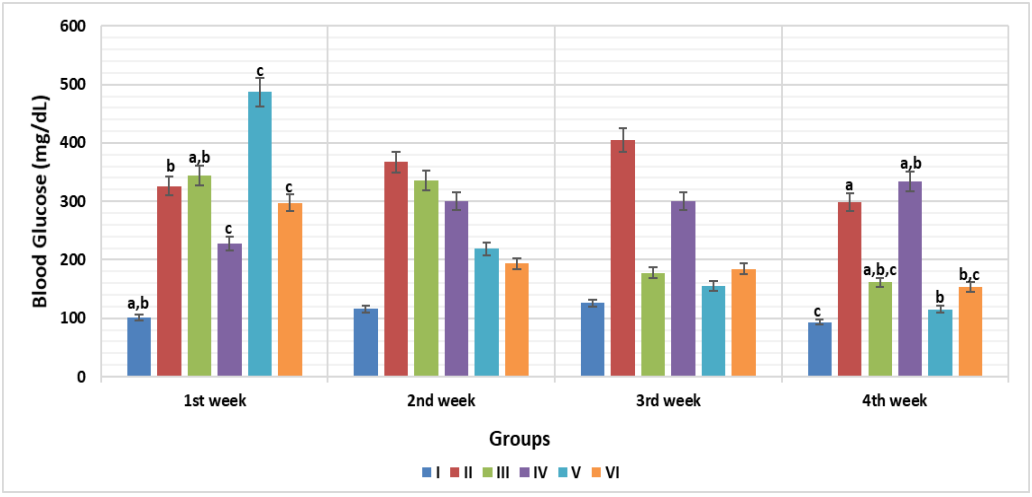

Figure 6. Changes in serum glucose (mg/dl) of rats with induced T2D and normal rats treated for 4 weeks after STZ administration where means that do not share a letter are significantly different. I: non-treated non-diabetic group (normal control), II: non-treated diabetic group (negative control), III: diabetic group treated with EEP, IV: diabetic group treated with CS-PAA nanoparticles, V: diabetic group treated with (EEP) conjugated with (CS-PAA) nanoparticles, VI: diabetic group treated with metformin

The findings of the current study illustrated that the blood glucose levels in T2DM rats were significantly higher than those in normal ones ($P<0.05$). These findings supported those of previous studies which concluded that healthy rats fed on a high-fat diet and later injected with low-dose STZ developed insulin resistance. In addition, hyperglycemia was later induced due to the aforementioned insulin resistance, and not due to a reduced insulin secretion, according to the findings of Li *et al.* [37].

The group of diabetic rats treated with EEP and EEP conjugated CS-PAA nanoparticles showed significantly reduced blood glucose levels from week 1 till the end of the treatment period. These findings were in agreement with the results of El Rabey *et al.* [35] and Kurek-Górecka *et al.* [38], who found that the oral administration of propolis to diabetic rats for 4 weeks expressively reduced glucose levels. The decrease in the blood glucose levels could have been a consequence of some bioactive constituents of propolis that had a protective effect on pancreatic β-cells as suggested in the study of Usman *et al.* [25] or due to increased peripheral utilization of glucose by direct stimulation of glucose uptake and inhibition of glucose transporter activity from the intestine, as proposed by Jadhav and Puchchakayala [39]. Past research suggested that propolis contains bioactive elements such as phenolic acids with hypoglycemic properties, and also indicated that propolis could improve blood glucose levels by promoting insulin secretion *in vivo* in STZ-induced diabetic rats [11].

In addition, treatment of diabetic rats with EEP conjugated CS-PAA nanoparticles for 4 weeks significantly decreased blood glucose levels by nearly three-folds compared with the untreated diabetic rats. This result came in agreement with Rivera-Yañez *et al*. [1]. Consequently, the results displayed that EEP conjugated with CS-PAA nanoparticles could almost regulate the hyperglycemia in the STZ-induced diabetic rats. The glycemic control realized by EEP treatment could have been due to the stimulation of glucose uptake by peripheral tissues, prevention of its release in circulation, or decreased glucose captivation in the gut [40]. Other explanations were presented by Mohammed *et al*. [41] who suggested chitosan nanoparticles could effectively deliver the loaded drugs at specific sites by locally retaining the drug to permit an extended time for drug absorption.

4. Conclusions

In conclusion, findings from the present study suggest that propolis conjugated with CS**-**PAA nanoparticles show a promising potential to control blood glucose in type 2 diabetic rats**.** However, more research is still needed to estimate the long**-**term effects of the proposed nano**-**therapy using propolis as an alternative type**-**2**-**diabetes therapy**.**

5. Acknowledgements

The authors would like to thank the Dean of the Faculty of Science and the Head of Entomology Department, Ain Shams University for giving permission to carry out our experiments in the Faculty of Science, Ain Shams University.

References

[1] Rivera-Yañez, N., Rodriguez-Canales, M., Nieto-Yañez, O., Jimenez-Estrada, M., Ibarra-Barajas, M., Canales-Martinez, M.M. and Rodriguez-Monroy, M.A., 2018. Hypoglycaemic and antioxidant effects of propolis of Chihuahua in a model of experimental diabetes. *Evidence-based Complementary and Alternative Medicine*, 2018, https://doi.org/10.1155/2018/4360356

[2] El-Awady, M.S., El-Agamy, D.S., Suddek, G.M. and Nader, M.A., 2014. Propolis protects against high glucose-induced vascular endothelial dysfunction in isolated rat aorta. *Journal of Physiology and Biochemistry*, 70(1), 247-254.

[3] Al-Hariri, M.T., 2011. Propolis and its direct and indirect hypoglycemic effect. *Journal of Family and Community Medicine*, 18(3), 152-154.

[4] Zhang, J., Cao, X., Ping, S., Wang, K., Shi, J., Zhang, C., Zheng, H. and Hu, F., 2015. Comparisons of ethanol extracts of Chinese propolis (poplar type) and poplar gums based on the antioxidant activities and molecular mechanism. *Evidence-Based Complementary and Alternative Medicine*, 2015, https://doi.org/10.1155/2015/307594

[5] Ali, I., Lone, M.N., Suhail, M., Mukhtar, S.D. and Asnin, L., 2016. Advances in nanocarriers for anticancer drugs delivery. *Current Medicinal Chemistry*, 23(20), 2159-2187.

[6] Rizvi, S.A.A. and Saleh, A.M., 2018. Applications of nanoparticle systems in drug delivery technology. *Saudi Pharmaceutical Journal*, 26(1), 64-70.

[7] Pulgaron, E.R. and Delamater, A.M., 2014. Obesity and type 2 diabetes in children: Epidemiology and treatment. *Current Diabetes Reports*, 14(8), 508, https://doi.org/10.1007/s11892-014-0508-y

[8] U.S. Food and Drug Administration, 2019. *Statement of Janet Woodcock, MD, Director of FDA's Center for Drug Evaluation and Research, on Impurities found in Diabetes Drugs Outside the U.S. States*. Available at: https://www.fda.gov/news-events/press-announcements/statement-janet-woodcock-md-director-fdas-center-drug-evaluation-and-research-impurities-found

[9] Souza, E.A., Zaluski, R., Veiga, N. and Orsi, R.O., 2016. Effects of seasonal variations and collection methods on the mineral composition of propolis from *Apis mellifera* Linnaeus Beehives. *Brazilian Journal of Biology*, 76(2), 396-401.

[10] Cunha, I.B.S., Sawaya, A.C.H.F., Caetano, F.M., Shimizu, M.T., Marcucci, M.C., Drezza, F.T., Povia, G.S. and Carvalho, P. de O., 2004. Factors that influence the yield and composition of Brazilian propolis extracts. *Journal of the Brazilian Chemical Society*, 15(6), 964-970.

[11] Usman, U.Z., Bakar, A.B.A. and Mohamed, M., 2016. Phytochemical composition and activity against hyperglycaemia of Malaysian propolis in diabetic rats. *Biomedical Research (India)*, 27(1), 46-51.

[12] Braun, D., Cherdron, H., Rehahn, M., Ritter, H. and Voit, B., 2013. *Polymer Synthesis: Theory and Practice.* Berlin: Springer-Verlag.

[13] Abou El Fadl, F.I., 2016. Synthesis and characterization of chitosan-poly(acrylamide-co-acrylic acid) magnetic nanocomposite hydrogels for use in catalysis. *Russian Journal of Applied Chemistry*, 89(10), 1673-1680.

[14] Ray, D., Mohanta, G.P., Manavalan, R. and Sahoo, P.K., 2009. Synthesis and characterization of acrylic based copolymeric hydrogel nanoparticles: An approach to drug delivery. *International Journal of ChemTech Research*, 1(3), 627-633.

[15] Wang, X., Chen, C., Huo, D., Qian, H., Ding, Y., Hu, Y. and Jiang, X., 2012. Synthesis of β-cyclodextrin modified chitosan-poly(acrylic acid) nanoparticles and use as drug carriers. *Carbohydrate Polymers*, 90(1), 361-369.

[16] Kao, H.J., Lo, Y.L., Lin, H.R. and Yu, S.P., 2006. Characterization of pilocarpine-loaded

chitosan/Carbopol nanoparticles. *Journal of Pharmacy and Pharmacology*, 58(2), 179-186.
[17] Andrade, Â.L., Manzi, D. and Domingues, R.Z., 2006. Tetracycline and propolis incorporation and release by bioactive glassy compounds. *Journal of Non-Crystalline Solids*, 352(32-35), 3502-3507.
[18] Zhu, A., Luo, X. and Dai, S., 2009. Chitosan-poly(acrylic acid) complex modified paramagnetic Fe_3O_4 nanoparticles for camptothecin loading and release. *Journal of Materials Research*, 24(7), 2307-2315.
[19] Vatandoust, N., Rami, F., Salehi, A.R., Khosravi, S., Dashti, G., Eslami, G., Momenzaden, S. and Salehi, R., 2018. Novel high-fat diet formulation and streptozotocin treatment for induction of prediabetes and type 2 diabetes in rats. *Advanced Biomedical Research*, 7(1), 107, https://doi.org/10.4103/abr.abr_8_17
[20] Dranse, H.J., Waise, T.M.Z., Hamr, S.C., Bauer, P.V., Abraham, M.A., Rasmussen, B.A. and Lam, T.T., 2018. Physiological and therapeutic regulation of glucose homeostasis by upper small intestinal PepT1-mediated protein sensing. *Nature Communications*, 9, 1118, https://doi.org/10.1038/s41467-018-03490-8
[21] Zhang, F., Ye, C., Li, G., Ding, W., Zhou, W., Zhu, H., Chen. G., Luo, T., Guang, M. Liu, Y., Zhang, D., Zheng, S., Yang, J., Gu, Y., Xie, X. and Luo, M., 2003. The rat model of type 2 diabetic mellitus and its glycometabolism characters. *Experimental Animals*, 52(5), 401-407.
[22] Sendrayaperumal, V., Pillai, S.I. and Subramanian, S., 2014. Design, synthesis and characterization of zinc-morin, a metal flavonol complex and evaluation of its antidiabetic potential in HFD-STZ induced type 2 diabetes in rats. *Chemico-Biological Interactions*, 219, 9-17.
[23] Motyl, K. and McCabe, L.R., 2009. Streptozotocin, Type I diabetes severity and bone. *Biological Procedures Online*, 11, 296-315.
[24] Al-Hariri, M., Eldin, T. and Al-Harb, M., 2016. Protective effect and potential mechanisms of propolis on streptozotocin-induced diabetic rats. *Journal of Taibah University Medical Sciences*, 11(1), 7-12.
[25] Usman, U.Z., Bakar, A.B.A. and Mohamed, M., 2018. Propolis improves pregnancy outcomes and placental oxidative stress status in streptozotocin-induced diabetic rats. *BMC Complementary and Alternative Medicine*, 18(1), 324, https://doi.org.//10.1186/s12906-018-2391-6
[26] Huang, S., Zhang, C.-P., Wang, K., Li, G. and Hu, F.-L., 2014. Recent advances in the chemical composition of propolis. *Molecules*, 19(12), 19610-19632.
[27] Huang, X.-Y, Guo, X.-L, Luo, H.-L, Fang, X.-W, Zhu, T.-G, Zhang, X.-L., Chen, H.W. and Luo, L.-P., 2015. Fast differential analysis of propolis using surface desorption atmospheric pressure chemical ionization mass spectrometry. *International Journal of Analytical Chemistry*, 2015, https://doi.org/10.1155/2015/176475
[28] Cevher, E., Salomon, S.K., Makrakis, A., Li, X.W., Brocchini, S. and Alpar, H.O., 2015. Development of chitosan-pullulan composite nanoparticles for nasal delivery of vaccines: Optimisation and cellular studies. *Journal of Microencapsulation*, 32(8), 755-768.
[29] Seven, P.T., Seven, I., Baykalir, B.G., Mutlu, S.I. and Salem, A.Z.M., 2018. Nanotechnology and nano-propolis in animal production and health: an overview. *Italian Journal of Animal Science*, 17(4), 921-930.
[30] Omidirad, R., Rajabi, F.H. and Farahani, B.V., 2013. Preparation and in vitro drug delivery response of doxorubicin loaded PAA coated magnetite nanoparticles. *Journal of the Serbian Chemical Society*, 78(10), 1609-1616.
[31] Guo, L., Liu, G., Hong, R.Y. and Li, H.Z., 2010. Preparation and characterization of chitosan poly(acrylic acid) magnetic microspheres. *Marine Drugs*, 8(7), 2212-2222.
[32] Dounighi, N.M., Eskandari, R., Avadi, M.R., Zolfagharian, H., Sadeghi, A.M.M. and Rezayat, M., 2012. Preparation and in vitro characterization of chitosan nanoparticles containing

Mesobuthus eupeus scorpion venom as an antigen delivery system. *The Journal of Venomous Animals and Toxins including Tropical Diseases*, 18(1), 44-52.

[33] Hussein, U., Hassan, N.Y., Elhalwagy, M.E.A., Zaki, A.R., Abubakr, H.O., Venkata, K.C.N., Jang, K.Y. and Bishayee, A., 2017. Ginger and propolis exert neuroprotective effects against monosodium glutamate-induced neurotoxicity in rats. *Molecules*, 22(11), 1928, https://doi.org/10.3390/molecules 22111928

[34] Peres, R.S., Zmozinski, A.V., Brust, F.R., Macedo, A.J., Armelin, E., Alemán, C. and Ferreira, C.A., 2018. Multifunctional coatings based on silicone matrix and propolis extract. *Progress in Organic Coatings*, 123, 223-231.

[35] El Rabey, H.A., Al-Seeni, M.N. and Bakhashwain, A.S., 2017. The antidiabetic activity of *Nigella sativa* and propolis on streptozotocin-induced diabetes and diabetic nephropathy in male rats. *Evidence-Based Complementary and Alternative Medicine*, 2017, https://doi.org/ 10.1155/2017/5439645

[36] Holmes, A., Coppey, L.J., Davidson, E.P. and Yorek, M.A., 2015. Rat models of diet-induced obesity and high fat/low dose streptozotocin type 2 diabetes: Effect of reversal of high fat diet compared to treatment with Enalapril or Menhaden oil on glucose utilization and neuropathic endpoints. *Journal of Diabetes Research*, 2015, https://doi.org/10.1155/2015/307285

[37] Li, Y., Chen, M., Xuan, H. and Hu, F., 2012. Effects of encapsulated propolis on blood glycemic control, lipid metabolism, and insulin resistance in type 2 diabetes mellitus rats. *Evidence-Based Complementary and Alternative Medicine*, 2012, https://doi.org/10.1155/ 2012/981896

[38] Kurek-Górecka, A., Rzepecka-Stojko, A., Górecki, M., Stojko, J., Sosada, M. and Świerczek-Zięba, G., 2013. Structure and antioxidant activity of polyphenols derived from propolis. *Molecules*, 19(1), 78-101.

[39] Jadhav, R. and Puchchakayala, G., 2012. Hypoglycemic and antidiabetic activity of flavonoids: Boswellic acid, Ellagic acid, Quercetin, Rutin on streptozotocin-nicotinamide induced type 2 diabetic rats. *International Journal of Pharmacy and Pharmaceutical Sciences*, 4(2), 251-256.

[40] Al-Hariri, M., Eldin, T.G., Abu-Hozaifa, B. and Elnour, A., 2011. Glycemic control and anti-osteopathic effect of propolis in diabetic rats. *Diabetes, Metabolic Syndrome and Obesity: Targets and Therapy*, 4, 377-384.

[41] Mohammed, M.A,, Syeda, J.T.M., Wasan, K.M. and Wasan, E.K., 2017. An overview of chitosan nanoparticles and its application in non-parenteral drug delivery. *Pharmaceutics*, 9(4), 53, https//doi.org//10.3390/pharmaceutics9040053